Interannual Variability of Summer Monsoon Onset over the Western North Pacific and the Underlying Processes

RENGUANG WU AND BIN WANG

Department of Meteorology and International Pacific Research Center, School of Ocean and Earth Science and Technology, University of Hawaii at Manoa, Honolulu, Hawaii

(Manuscript received 10 May 1999, in final form 11 October 1999)

ABSTRACT

Climatological summer monsoon onset over the South China Sea (SCS) and the western North Pacific (WNP) (defined as the region of 10°–20°N, 120°–160°E) displays three distinct stages. Around mid-May, monsoon rain commences in the SCS and the Philippines. In early to mid-June, the monsoon rain extends to the southwestern Philippine Sea. After mid-July, the rainy season starts in the northeastern part of the WNP. The onset anomaly, however, displays an in-phase interannual variation across the entire WNP domain. The standard deviation of the onset date increases eastward from 3 pentads in the SCS to 5 pentads in the northeastern part of the domain. The large onset variability in the WNP is mainly attributed to large year-to-year changes of the seasonal cycle. The role of the intraseasonal oscillation is secondary but important especially in the SCS region. The El Niño–Southern Oscillation (ENSO)-related thermal contrast between the WNP and the equatorial central Pacific modulates significantly the seasonal migration of the monsoon trough, the subtropical high, and the convection zone over the WNP during late spring–early summer in the ENSO decay phase. Thus, ENSO plays a dominant role in the interannual variation of the WNP summer monsoon onset.

The general circulation model results suggest that during El Niño events, the warm SST anomalies in the equatorial eastern-central Pacific play a major role in generation of large-scale upper-level convergence and descent anomalies over the WNP. Meanwhile, the cold SST anomalies in the WNP induce lower-level anticyclonic wind anomalies and reduce convective instability. Both the remote and local SST forcing are important for delaying the seasonal movement of the monsoon trough and the western Pacific subtropical high and hence the onset of the monsoon rain. In the La Niña case, the local warm SST anomalies in the WNP are more important than the cold SST anomalies in the equatorial eastern-central Pacific in the generation of lower-level cyclonic wind anomalies and enhancement of convective instability.

1. Introduction

The western North Pacific summer monsoon (WNPSM) is an important subcomponent of the Northern Hemisphere summer monsoon. The convective activity over the western North Pacific (WNP) displays pronounced interannual variability and has considerable impacts on weather and climate over East Asia (Nitta 1987). The related sea surface temperature (SST) changes in the WNP may act as a linkage between the El Niño–Southern Oscillation (ENSO) and the East Asian summer monsoon (Huang and Wu 1989; Shen and Lau 1995).

The onset time of the WNPSM appears to have much larger interannual variability compared to the Indian summer monsoon (Murakami and Matsumoto 1994). It is not well known what causes this difference. In the South China Sea (SCS), the onset also exhibits a large year-to-year change (Lau and Yang 1997) with an interannual range of about one month (Yan 1997). Wang and Wu (1997) pointed out that the interannual variation of the SCS summer monsoon onset exhibits two principal modes: a normal mode (onset occurring in mid-May) and a delayed mode. The absence of the early onset is due to a prominent dry singularity occurring in early May over the SCS.

Tanaka (1997) noticed the late (early) onset of the WNPSM in El Niño (La Niña) years. The delayed (advanced) onset of the SCS summer monsoon was suggested to be related to the basinwide warm (cold) events of the Pacific Ocean (Lau and Yang 1997). It is unclear, however, what are the underlying processes responsible for the interannual variability of the onset in the SCS and WNP.

The relative roles of the seasonal cycle transition and the intraseasonal oscillation (ISO) in the interannual variation of the onset vary with locations. In Australia, both the seasonal cycle and the ISO are important in determining the timing of the summer monsoon onset, where-

Corresponding author address: Prof. Bin Wang, Department of Meteorology and International Pacific Research Center, University of Hawaii at Manoa, 2525 Correa Road, Honolulu, HI 96822.
E-mail: bwang@soest.hawaii.edu

as the ISO is more important than the seasonal cycle in determining the onset of the South Asian summer monsoon (Murakami et al. 1986). What are the relative roles of the seasonal cycle and the ISO in the interannual variation of the onset in the WNP? Clarification of this question will help to identify the causes and processes for the interannual variation of the WNPSM onset. It also helps the onset prediction.

Various hypotheses have been proposed to explain the onset variability in Indian and Australian monsoons. Hendon et al. (1989) proposed that the upward motion over the equatorial central Pacific due to ENSO-related warm SST induce subsidence over the Australian longitude, thus inhibiting the normal monsoon onset in northern Australia. Joseph et al. (1991) hypothesized that warm waters in the north Indian Ocean and cold waters north of Australia may delay the southeastward migration of convection from the Indian Ocean to northern Australia, which in turn results in a delayed onset of the Australian summer monsoon. The delayed onset at Kerala, the southern tip of India, was attributed to the El Niño-related positive SST anomalies in the equatorial central Pacific that delay the seasonal northwestward movement of the equatorial convective cloudiness maximum (Joseph et al. 1994). Positive SST anomalies in the south Indian Ocean and/or negative SST anomalies in the Arabian Sea may play a similar role. Based on numerical studies using an atmospheric general circulation model, Ju and Slingo (1995) and Soman and Slingo (1997) found that the influence of El Niño on the South Asian summer monsoon is through modulating the latitudinal position of the intertropical convergence zone over Indonesia in the preceding spring. How does the ENSO affect the WNPSM onset? Is it through the large-scale circulation changes induced by the SST anomalies in the equatorial central Pacific or through the lower-level circulation and thermodynamic changes induced by the local SST anomalies? What are the relative roles of remote and local SST forcing? These questions have not been addressed.

The interannual variability of the WNPSM onset has not been systematically studied. The aim of this study is to fill this gap. The objectives are to address the following questions. 1) What are the characteristics of the interannual variability of the WNSPM onset? 2) What are the important factors controlling the interannual variation of the WNPSM onset? 3) How is the interannual variation of the WNPSM onset related to tropical Pacific SST anomalies? 4) What processes advance or delay the WNPSM onset?

2. Data and definition of the onset

a. Data

Pentad and monthly mean outgoing longwave radiation (OLR) data on 2.5° × 2.5° grids with global coverage are constructed from daily means of the National Oceanic and Atmospheric Administration (NOAA) satellite observation spanning from 1975 to 1995 with a 9-month gap in 1978. The achieved OLR data have had some corrections made for changes in instruments and spectral windows (Gruber and Krueger 1984), but not for changes in the equatorial crossing time of different operating satellites. Previous studies pointed out the necessity to remove the OLR biases due to the equatorial crossing time changes before the dataset is used for the study of the interannual variations (e.g., Chelliah and Arkin 1992; Gadgil et al. 1992; Waliser and Zhou 1997). We made corrections for pentad and monthly mean OLR within 45°S–45°N to remove these OLR biases. The procedure used is similar to that by Waliser and Zhou (1997) who calibrated only monthly mean OLR within 30°S–30°N. To determine the bias pattern, we first identify the spurious spatial mode relating to diurnal variations involved in the changes of the equatorial crossing time. To retain only the changes in relation to slow drifts of the equatorial crossing time, we adjust the time coefficient for each time period between the abrupt changes of the equatorial crossing time using a second-order polynomial fitting to minimize the least square errors. We then multiply the artificial spatial pattern by the adjusted time series to determine approximately the bias pattern due to the equatorial crossing time changes.

The National Centers for Environmental Prediction–National Center for Atmospheric Research (NCEP–NCAR) reanalysis (Kalnay et al. 1996) provides daily mean atmospheric data with global coverage. Pentad and monthly means are constructed from daily means for the period of 1979–95. The wind, geopotential height, vertical motion, temperature, and specific humidity at multiple levels have a horizontal resolution of 2.5° × 2.5°. Latent heat flux and skin temperature are on Gaussian grids of T62 with a horizontal resolution of about 1.9° × 1.9°. Over the open ocean, the skin temperature is fixed at the Reynolds SST in the reanalysis (Kalnay et al. 1996).

Monthly mean SST data on 3° × 1° grids in the tropical Pacific for the period of 1980–95 are from NCEP's Ocean Data Assimilation System (Ji et al. 1995). Other SST data are Reynolds reconstructed monthly mean SSTs (Reynolds and Smith 1994; Smith et al. 1996) that has a global coverage between 45°S–60°N and a resolution of 2° × 2° spanning from 1950 to 1992. This dataset is used in constructing SST anomalies for our numerical experiments.

b. Seasonal cycle and intraseasonal oscillation

The monsoon onset is determined by both the seasonal cycle and the ISO. The seasonal cycle is a forced response and highly influenced by lower boundary conditions, whereas the ISO is of a more chaotic nature and determined primarily by the atmospheric internal dynamics. Separation of the two components thus facilitates physical discussions.

Harmonic analysis for multiyear pentad mean time series is employed to separate the two components. The seasonal cycle is reconstructed from the sum of the long-term mean and those harmonics with periods of 90 days or longer. The ISO component is represented using the sum of those harmonics with periods of 20–90 days. The defined seasonal cycle differs from the seasonal cycle in climatological sense. It incorporates the interannual variations and changes from year to year both in phase and amplitude. A limitation of the harmonic analysis is related to its linear decomposition that cannot resolve the interaction between the two components.

c. Definition of the onset

The fundamental features of monsoon are the annual wind reversal and dry and wet alternation. Thus, the summer monsoon onset is characterized by a sudden wind switch and a dry to wet transition. Locally, however, the wind switch and the dry to wet transition are not necessarily simultaneous. For example, many parts of northeastern and eastern India experience northwesterlies in premonsoon months of April and May (Das 1987). These winds are associated with violent thunderstorms. The 850-hPa westerly winds at the head of the Bay of Bengal start much earlier than the commencement of deep convection (Murakami and Matsumoto 1994). Similar situations occur in northern SCS and the northwestern Philippine Sea. The westerly winds there are related to midlatitude systems before the commencement of summer monsoon. Drosdowsky (1996) pointed out that on the timescale associated with the transition between active and break phases, no clear relationship is found between westerly winds and rainfall. He suggested that it is not a useful procedure to combine rainfall and wind into a single ''wet westerly'' monsoon onset definition. Physically, the discrepancies result from the dynamical structure of the monsoon systems. The wind and convection normally display a phase shift in space so that locally the wind switch and the flare-up of convection are not necessarily in phase. The inconsistencies between local wind switch and dry-to-wet transition pose a difficulty in defining the onset in the WNP by using both wind and rainfall (or OLR) at the same location (Wu 1999).

A traditional variable for the onset definition is rainfall. Over the ocean, there is no systematic rainfall observation. An alternative choice is OLR. The OLR has homogeneous spatial sampling, relatively high temporal and spatial resolution, and a full coverage over the Tropics. There are, however, contaminations from cirrus clouds, surface temperature, and atmospheric moisture content. It is hard to estimate the errors due to these contaminations. Previous estimation based on monthly means indicates a good relation between OLR and rainfall in the Tropics (Xie and Arkin 1998). On timescales less than one month, the relation may become worse due to the effects of high-frequency variations. Generally, the rainfall displays small-scale features in space and time due to the effects of local wind systems, such as land–sea breezes, the topographic effects, and the influences of synoptic events, such as tropical storms.

In this study, the monsoon onset is defined using pentad mean OLR. A simple definition for the onset would be the transition time at which the pentad mean OLR becomes lower than a threshold value, for example, 240 W m^{-2}. The selection of 240 W m^{-2} is subjective. It approximately corresponds to a rain rate of 6 mm day^{-1} in the WNP according to estimation based on climatological pentad mean OLR and Climate Prediction Center Merged Analysis of Precipitation (see Xie and Arkin 1997) in the WNP. A uniform threshold value is used in the present study because the monsoon domain is confined to the tropical ocean. If we consider that the diabatic heating is proportional to the rain rate and the atmospheric response depends on the diabatic heating, then a uniform threshold value would be preferred.

A practical difficulty encountered is the presence of more than one transition due to the ISO. Specifically, following the wet period after the first transition, there may be a dry period followed by a second transition. Consider two cases. In the first case, the wet period is stronger and longer than the following dry period. In the second case, the wet period is weaker and shorter than the following dry period. Since the onset refers to the transition to a persistent wet regime, it is reasonable to choose the first (second) transition as the onset in the first (second) case. On the other hand, the asymmetry of the wet and dry periods is associated with the seasonal cycle transition. The seasonal cycle transition (from above to below 240 W m^{-2}) is likely to occur in the wet (dry) period in the first (second) case. Thus, we use the seasonal cycle to make the selection when there are multiple transitions. The physical basis for this is that the seasonal evolution represents the establishment of large-scale circulation and thermodynamics for the monsoon.

Since the monsoon onset refers to the transition to a sustained wet regime, we neglect the effects of high-frequency variations (period <20 days). Inclusion of the high-frequency variations will produce some small-scale features in the onset pattern but will not affect the large-scale characteristics. To reduce the influence of local wind systems and synoptic events, pentad means averaged on $5^\circ \times 5^\circ$ boxes are used in the determination of onset pentad at the center of the box. The onset is defined as the first pentad after March during which OLR satisfies the following two criteria. 1) Pentad mean OLR transits from above to below 240 W m^{-2} (pentad mean transition). 2) The seasonal cycle of OLR transits to below 240 W m^{-2} during the wet period following the pentad mean transition.

3. Climatology and interannual variation of the monsoon onset in the WNP

The WNP has large annual range of OLR (Murakami and Matsumoto 1994) and clear signal of seasonal wind

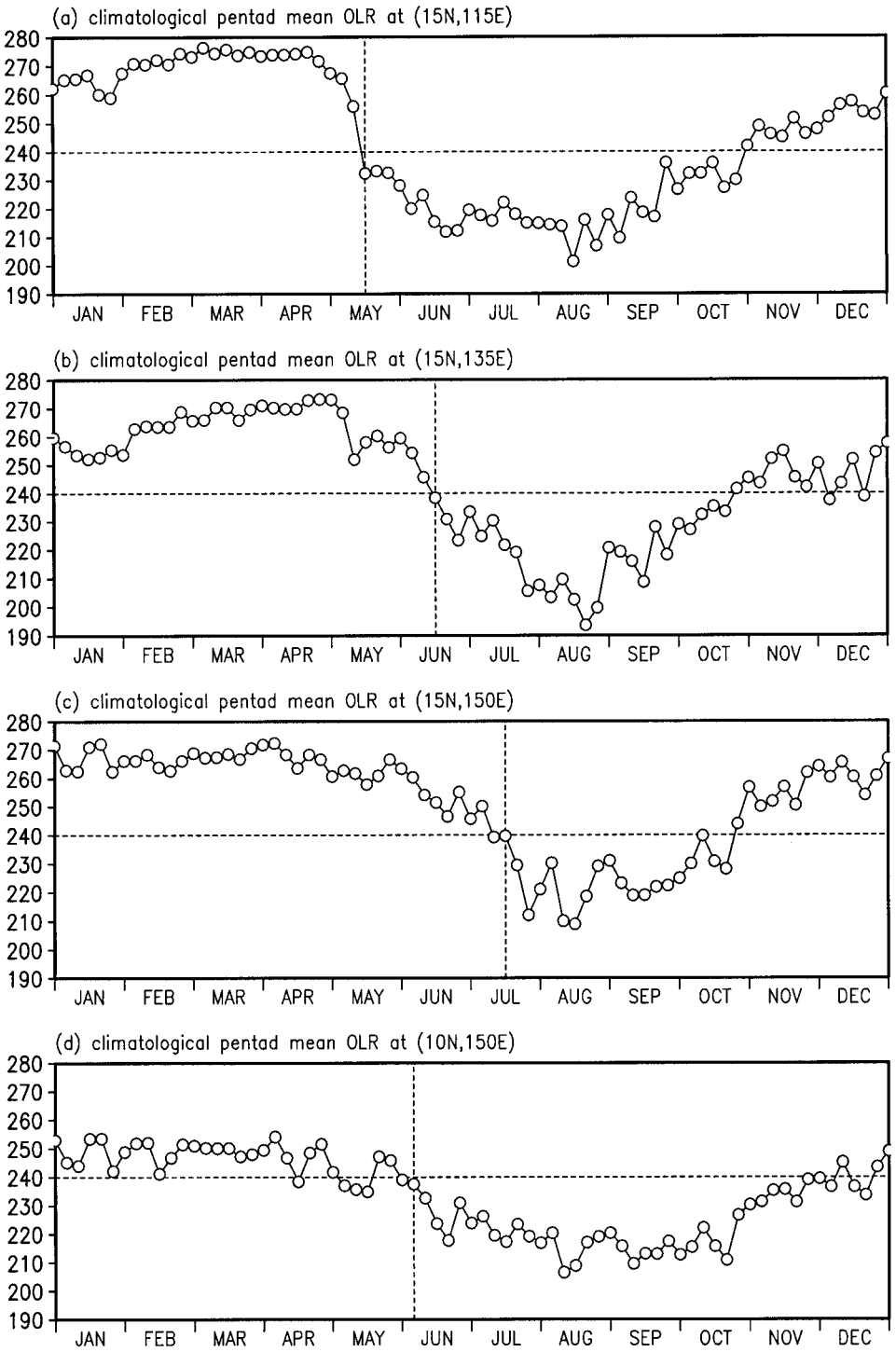

FIG. 1. Time series of climatological pentad mean OLR (W m^{-2}) at (a) 15°N and 115°E, (b) 15°N and 135°E, (c) 15°N and 150°E, (d)10°N and 150°E. The dashed vertical lines indicate the onset dates.

reversal (Wu 1999). The June–October (taken approximately as the monsoon period in the WNP, see Fig. 1) rainfall accounts for 60%–75% of the yearly total rainfall over the region of 10°–20°N, 110°–160°E. The climatological pentad mean OLR shows a clear transition from the dry to the wet regime (Fig. 1). The wet regime is sustained after the onset. Pronounced circulation changes are also observed at the onset (Wu 1999). Thus, the WNP displays typical monsoon character.

This study focuses on the monsoon region between

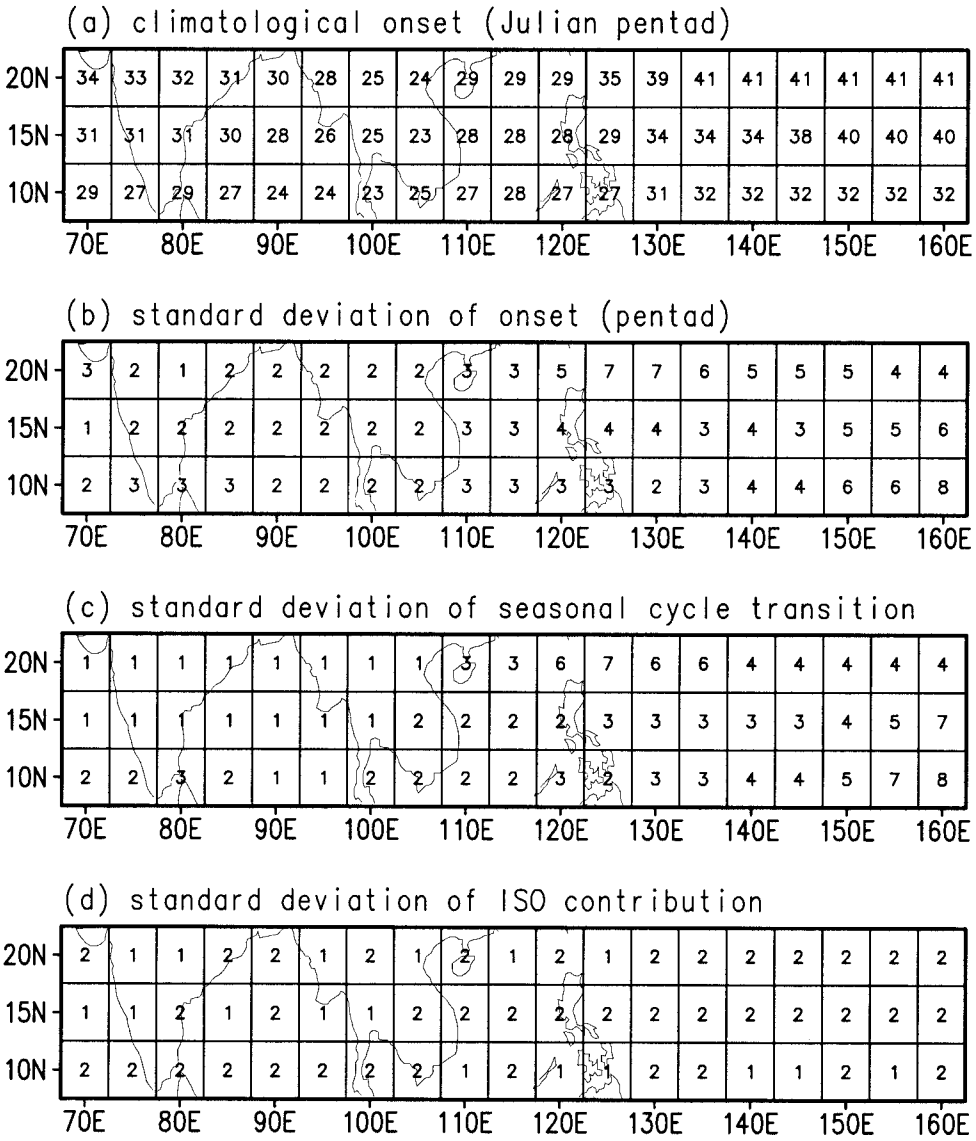

FIG. 2. (a) Climatological summer monsoon onset pentad, (b) the standard deviation of the onset, (c) the standard deviation of the seasonal cycle transition, and (d) the standard deviation of the ISO contribution to the onset.

10° and 20°N extending from 110° eastward to 160°E. This region is slightly larger than the domain defined by Murakami and Matsumoto (1994). Cautions should be applied to the region east of 145°E and along 10°N where the onset in individual years may not be detected according to the criteria. Figure 2a displays climatological onset determined using climatological pentad mean OLR. In this case, the separation of the seasonal cycle and the ISO is based on harmonic analysis applied to climatological pentad mean time series. In Fig. 2a, the onset occurs first in the Indochina peninsula in pentad 23–25 (21 April–5 May) between 10°–20°N. The onset occurs progressively later northwestward through the Bay of Bengal to the Indian subcontinent. It reaches northwestern India after pentad 33 (10–14 June). The gross feature of the onset advance in the Indian monsoon region resembles that of Indian Meteorological Department (1943) and Murakami and Matsumoto (1994). In the Indochina peninsula, the defined onset is close to Matsumoto (1997), but earlier than Lau and Yang (1997) who used 6 mm day^{-1} of rain rate as the threshold for the onset.

The onset progresses eastward through the SCS (pentad 27–28, 11–20 May), southwestern Philippine Sea (pentad 32–34, 5–19 June) and to the northeastern part of the domain (pentad 40–41, 15–24 July). The gross trend of the onset advance is consistent with that of Wang (1994) who considered only the annual and semiannual harmonics of pentad mean OLR. The onset dates in the SCS and southwestern Philippine Sea are similar

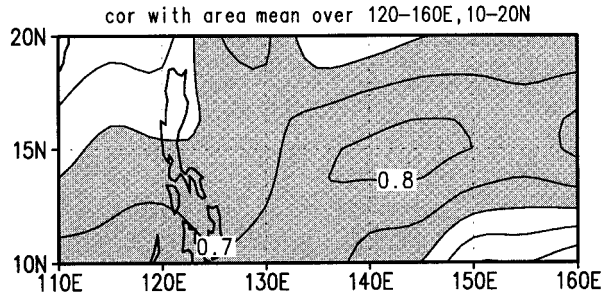

FIG. 3. Correlation of the onset at each 5° × 5° grid with the onset averaged over 10°–20°N, 120°–160°E during 1975–95 (except 1978). Shaded regions are for correlation coefficients over 0.6.

to Murakami and Matsumoto (1994). In the northeastern part of the domain, the onset dates are much earlier than those in Murakami and Matsumoto (1994) because they used local annual mean OLR as the threshold that changes from place to place. In the northeastern part of the domain, the annual mean OLR exceeds 250 W m^{-2}. Taking such a threshold apparently yields an earlier onset date. The onset in the SCS and northwestern Philippine Sea is much earlier than Tanaka (1992) who used the 30% of mean high cloud amount as a threshold to define the onset.

An important feature in the climatological onset (Fig. 2a) is that the northeastward advance of the onset is stepwise. Three distinct stages can be identified in the SCS and the WNP. In the first stage, the onset occurs in the SCS and the Philippines with a relatively uniform onset time between pentad 27 (11–15 May) and pentad 29 (21–25 May). In the second stage, the onset takes place in the southwestern Philippine Sea from pentad 32 (5–9 June) to pentad 34 (15–19 June). In the third stage, the onset reaches northeastern part around pentad 40–41 (15–24 July).

Figure 2b shows the standard deviation of the onset. The standard deviation exceeds 3–4 pentads in the SCS and the WNP. That is twice larger than that in the Indian monsoon region where the standard deviation is about 2 pentads. The largest year-to-year variability of the onset is found in the southeast corner and to the northeast of the Philippines. The former is located at the margin of the monsoon domain where the annual range is small. The latter is in the subtropical side of the domain where the effects from midlatitude systems are considerably large. There is a general increasing tendency of the standard deviation from 2 pentads in the Indian subcontinent through the Indochina peninsula, to 3 pentads in the SCS, 3–4 pentads in the southwestern Philippine Sea, and 4–5 pentads in the northeastern part of the domain.

A prominent feature of the interannual variation is that the onset anomalies in the WNP are nearly in phase. This can be seen from Fig. 3 that shows the correlation of the onset anomaly at each grid with the area-mean onset anomaly over 10°–20°N, 120°–160°E. High correlation over 0.6, which is significant over 95% confidence level, covers most of the domain except northern SCS and the southeast corner. This indicates that the onset anomaly has an in-phase interannual variation across the entire domain. In most of the years, the onset anomaly in the WNP is dominated by either early-to-normal or late-to-normal onset (figures not shown).

4. Roles of the seasonal cycle and the intraseasonal oscillation

Figure 2c shows the standard deviation of the seasonal cycle transition time that measures the contribution of the seasonal cycle to the interannual variation of the onset. In the Indian monsoon region (70°–105°E), the standard deviation is only about 1 pentad except along 10°N in the vicinity of the southern tip of India. This indicates that the seasonal cycle transition in the Indian monsoon region is quite ''punctuated'' and has little interannual variation. In the SCS region, the standard deviation is about 2 pentads, twice that in the India monsoon region. From the SCS moving northeastward, the standard deviation increases systematically from 2 to 4 pentads. In the Philippine Sea, the variability of the seasonal cycle transition time is 3–4 times of that in the India monsoon region. The northeastward increase of the standard deviation corresponds well to the progressively later onset in the SCS and WNP (Fig. 2a). In other words, in the SCS, the southwestern Philippine Sea, and the northeastern part of the domain, the onset occurs in mid-May, mid-June, and late July, respectively, whereas the standard deviation of the seasonal cycle transition time amounts to 2, 3, and 4 pentads, respectively. The largest onset variability is found in the northeast of the Philippines and the southeast corner of the domain where the standard deviation reaches 6–7 pentads. We speculate that in the former region the onset is sensitive to the activity of midlatitude systems, whereas in the latter region the annual cycle is weak and the onset is sensitive to the large interannual variation of SST.

Figure 2d shows the standard deviation of the difference between the onset and the seasonal cycle transition time. This difference is caused by the ISO. Thus, it reflects the onset variability induced by the ISO. Note that the ISO-induced onset variability is about 2 pentads across the entire domain. This is not surprising since the ISO has a typical period of about 6 pentads. When it is superimposed on the seasonal cycle, its wet and dry phases can normally shift the onset from the seasonal cycle transition time by about 2 pentads.

Comparison of Figs. 2c and 2d indicates that in the Indian monsoon region, the year-to-year variability of the onset is largely attributed to the ISO, consistent with Murakami et al. (1986). Prediction of the onset in the Indian monsoon region thus requires an accurate prediction of the ISO. In the SCS region, the seasonal cycle and the ISO has roughly the same contribution to the

onset variability. Thus, both of them are important in the prediction of the onset. The seasonal cycle plays a more important role than the ISO in the WNP. Especially in northeastern part of the domain, about two-thirds of the onset variability can be accounted for by the seasonal cycle.

In summary, the relative role of the seasonal cycle versus the ISO in the onset variability increases eastward from India to the WNP tremendously. This is because the seasonal cycle transition is tightly locked with calendar dates in South Asia but is progressively less locked eastward. In this sense, the marine monsoon is much more variable than the continental monsoon. The small variation of the seasonal cycle transition time in South Asia is primarily due to the land heating effect. Geographically fixed land forcing makes the phase of the seasonal cycle change little from year to year under regular seasonal evolution of solar radiation. This may be enhanced by the massive Tibetan Plateau to the north. The variable seasonal cycle transition in the WNP is related to the large variation of SST in relation to ENSO that is much more variable from year to year compared to the land surface heating.

5. Relation of the interannual variation of the onset to SST anomalies

The onset anomaly distribution in individual years displays a large-scale feature in the WNP (Fig. 3). Thus, it is meaningful to examine the area-mean onset anomaly and its relation to SST anomalies. The onset anomaly averaged over 10°–20°N, 120°–160°E is shown in Fig. 4a, along with the onset anomalies averaged over three subregions: 10°–15°N, 110°–120°E; 10°–15°N, 130°–140°E; and 15°–20°N, 145°–155°E. The three subregions are selected according to the three stages of the onset. General consistence can be identified for the interannual variation of the onset. This further demonstrates the large-scale coherent feature of the onset anomaly in the WNP.

Figure 5 shows the correlation between the area-mean onset anomaly over 10°–20°N, 120°–160°E and the SST anomalies in the tropical Pacific during 1980–95. High positive and negative correlations are found in the equatorial eastern-central Pacific and WNP, respectively. These high correlations persist from winter to June. They decrease quickly after July. Similar correlation distributions are obtained when the onset anomaly is averaged over the three subregions.

The correlation distribution indicates that in the late onset years, there are positive SST anomalies in the equatorial eastern-central Pacific and negative SST anomalies in the WNP. Opposite SST anomalies are observed in the early onset years. This is confirmed by contrasting the composite SST anomaly distribution in the late and early onset years (figures not shown). The distinct SST anomaly patterns in the late and early onset years suggest that the large-scale SST anomaly pattern in the tropical Pacific Ocean is probably a fundamental factor leading to the anomalous onset of the WNPSM.

An SST index is constructed to reflect the thermal contrast between the equatorial central Pacific and the WNP. The index is defined as the difference of normalized area-mean SST anomalies in March–May between the equatorial central Pacific (5°S–5°N, 180°–140°W) and the east of the Philippine Sea (10°–15°N, 140°–160°E). The equatorial central Pacific is selected because it is located at the eastern bound of the western Pacific warm pool and exhibits a large zonal SST gradient in climatology. The east–west shift of the warm pool and convection along the equator is sensitive to the SST anomalies in this region. The region of 10°–15°N, 140°–160°E is located slightly to the southeast of the core region of the WNPSM (10°–20°N, 130°–150°E). Its selection is based on the fact that the large SST anomalies in the WNP tend to be located to the southeast of anomalous convection. We take the spring because that is the time when the western Pacific warm pool moves from southeast to northwest. The SST anomalies in spring impact the seasonal march of warm pool. Even so, a question may be raised as to why not to use winter SST anomalies to construct the SST index that has more prediction value. Whether the winter or spring SST index is used, the classification for composite analysis in the next section based on the SST index will not change since the SST anomalies usually persist from winter to spring. However, the direct effect on circulation anomalies in the preonset season comes from the spring SST anomalies.

The constructed SST index is displayed in Fig. 4b. The respective SST anomalies in the two regions are also shown (Fig. 4c). It is seen that the index can represent well the SST anomalies in the two regions. High (low) SST index corresponds to positive (negative) SST anomalies in the equatorial central Pacific and negative (positive) SST anomalies in the WNP. The correlation of the SST index with Niño-3 SST anomalies in northern spring is about 0.89 during 1980–95, indicating a close relation of the defined index with ENSO. Comparison of Figs. 4a and 4b indicates a good correspondence in the interannual variation of the onset and the SST index. The high SST index values in 1983, 1987, 1992, and 1993 correspond to the late onset in the large area of the WNP, whereas the low SST index values in 1981, 1984, 1985, 1986, 1988, and 1989 are followed by the early onset.

6. Changes of large-scale circulation and thermal structure during the onset

To understand how the large-scale SST anomaly pattern in the tropical Pacific affects the WNPSM onset, we examine the large-scale circulation and thermodynamic changes. Two types of composites were made based on the SST index. One is high SST index over 1.0 (1983, 1987, 1992, and 1993). The other is low SST

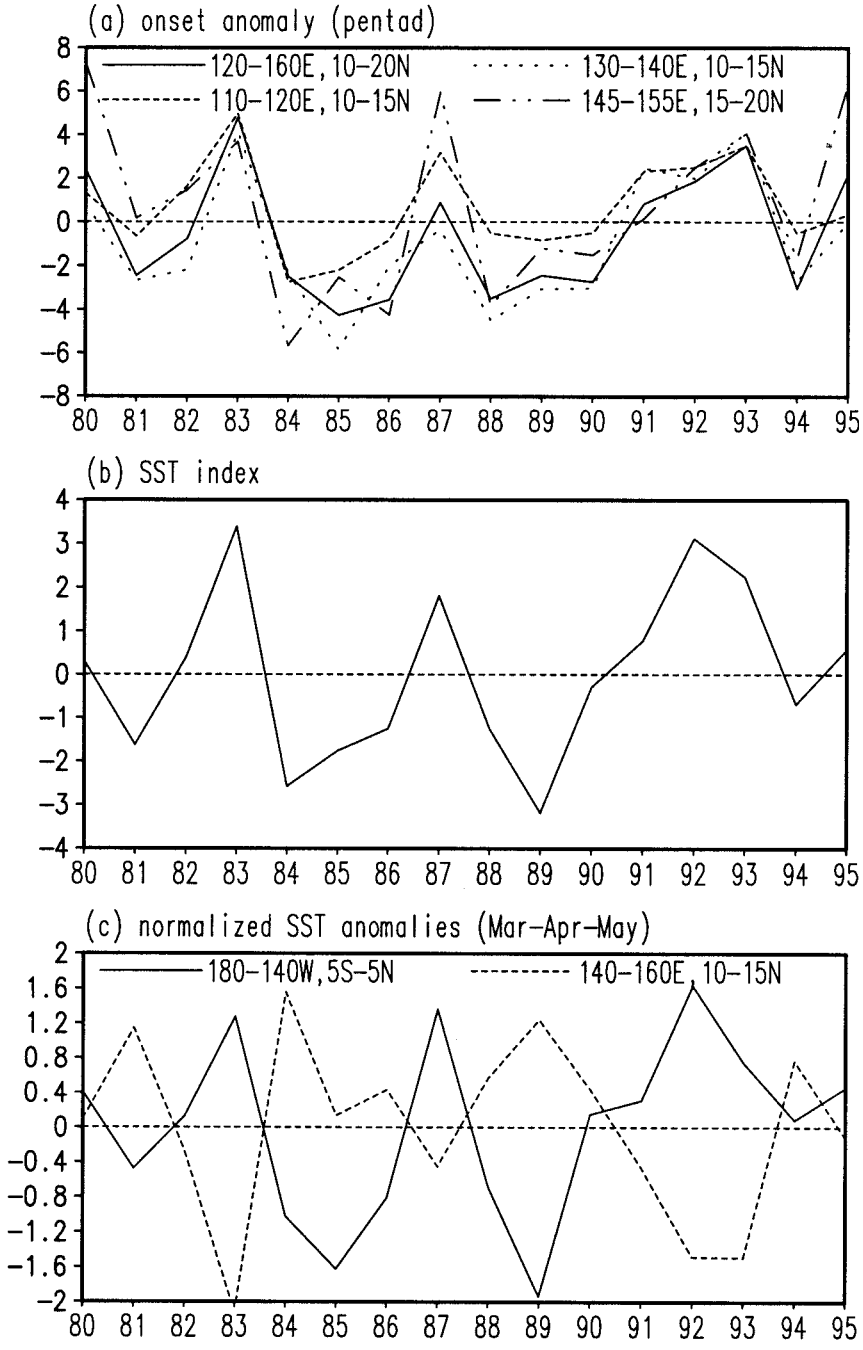

FIG. 4. (a) Onset anomaly averaged over the following regions: 10°–20°N, 120°–160°E; 10°–15°N, 110°–120°E; 10°–15°N, 130°–140°E; and 15°–20°N, 145°–155°E. (b) SST index defined as the difference between the solid curve and dashed curve in (c). (c) Normalized area-mean SST anomalies in Mar–May for the regions of 5°S–5°N, 180°–140°W (solid curve) and 10°–15°N, 140°–160°E (dashed curve), respectively.

index below −1.0 (1981, 1984, 1985, 1986, 1988, and 1989). In the following, the discussion will focus on the composites in high SST index years since the composites in low SST index years are basically of opposite features.

The large-scale SST anomaly pattern in the tropical Pacific induces important changes in the atmospheric circulation over the WNP. In the high SST index years, there are anomalous upper-level convergence, deep descent with a maximum at 300–400 hPa, and boundary layer divergence (Fig. 6, top panels). The 200-hPa cyclonic and the boundary layer anticyclonic vorticity

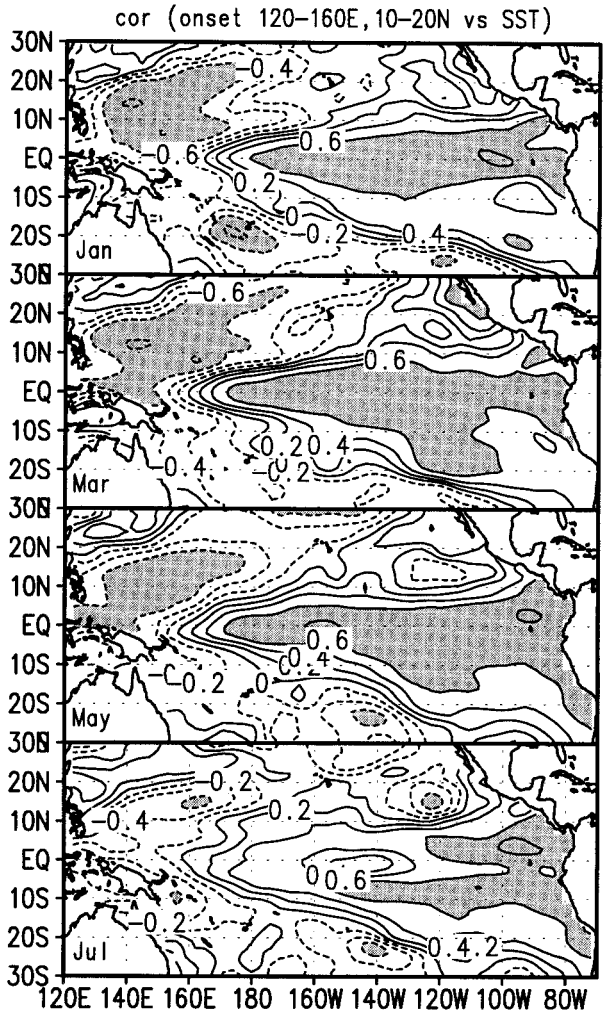

FIG. 5. Correlation maps of the onset anomaly averaged over the WNP (10°–20°N, 120°N–160°E) with SST anomalies in Jan, Mar, May, and Jul during 1980–95. Shaded regions are for correlation coefficients exceeding 0.6 that are significant over 95% confidence level according to an estimation of the decorrelation time (Livezey and Chen 1983).

anomalies are evident. Opposite anomalies occur in the low SST index years with smaller amplitudes especially in the vorticity field.

The local SST anomalies may influence atmospheric moisture and temperature through surface heat fluxes and turbulent mixing in the boundary layer. The circulation changes induced by both remote and local SST anomalies also impact temperature and moisture. In the high SST index composite, the large anomalous boundary layer moisture divergence reduces the lower-level moisture (Fig. 6, bottom panels). The negative temperature anomaly decreases with height from 850 to 600 hPa. The moisture and temperature changes indicate a decrease of convective instability. Opposite anomalies occur in the low SST index years.

To show the evolution of circulation and convection anomalies and their relation to SST anomalies, we present, in Fig. 7, the differences in SST, 850-hPa winds, and OLR between the high and low SST index years during May–July. The anomalies in the high SST index years are similar to the differences and those in the low SST index years are basically opposite to the differences. In Fig. 7a, the 28°C SST contour in climatology is plotted to outline the regions where deep convection may occur (e.g., Gadgil et al. 1984; Graham and Barnett 1987). The 240 W m^{-2} OLR contour on Fig. 7c represents regions of large-scale convection in climatology.

The western Pacific warm pool (SST exceeding 28°C) expands northeastward in the WNP from May to July (Fig. 7a). In the high SST index years, the presence of warm SST anomalies in the equatorial eastern-central Pacific indicates that the warm pool shifts eastward along the equator. In the WNP, the warm pool shifts southwestward compared to climatology as implied by the negative SST anomalies. Thus, in the high SST index years, the northeastward seasonal march of the warm pool is delayed in late spring to summer. On the contrary, it is earlier than normal in the low SST index years.

In climatology, the monsoon trough is located in the SCS in May (Fig. 7b). It migrates eastward across the Philippine archipelago in June. In July, the trough moves farther northeastward. In the high SST index years, due to the presence of anticyclonic wind anomalies over the SCS and WNP, the monsoon trough is located to the west in May and southwest in June and July compared to climatology. Thus, the seasonal progress of the monsoon trough is delayed in the high SST index years. Opposite situation occurs in the low SST index years.

A noticeable feature in Fig. 7b is that the anomalous lower-level anticyclone over the SCS and WNP moves northeastward with the season. These wind anomalies reflect changes in the seasonal movement of the WNP subtropical high. In the high SST index years, the subtropical high is stronger than normal and located at lower latitudes compared to climatology as indicated by positive height anomalies at lower latitudes and the equatorward extension of the 5870-m contour (Fig. 8a), consistent with anomalous downward motion in the WNP (Fig. 6). In the low SST index years, the opposite feature is observed (Fig. 8b). Thus, the WNP subtropical high displays a delayed (advanced) seasonal northward movement in the high (low) SST index years.

The induced convection anomalies are demonstrated in Fig. 7c. Climatologically, the convection zone in the WNP moves northeastward from May to July. In the high SST index years, there are negative OLR anomalies in the equatorial eastern-central Pacific and positive OLR anomalies in the SCS and WNP. The positive OLR anomalies display obvious northeastward displacement from May to July, consistent with the movement of the lower-level anomalous anticyclone (Fig. 7b). The OLR anomalies in the WNP indicate that the northeastward

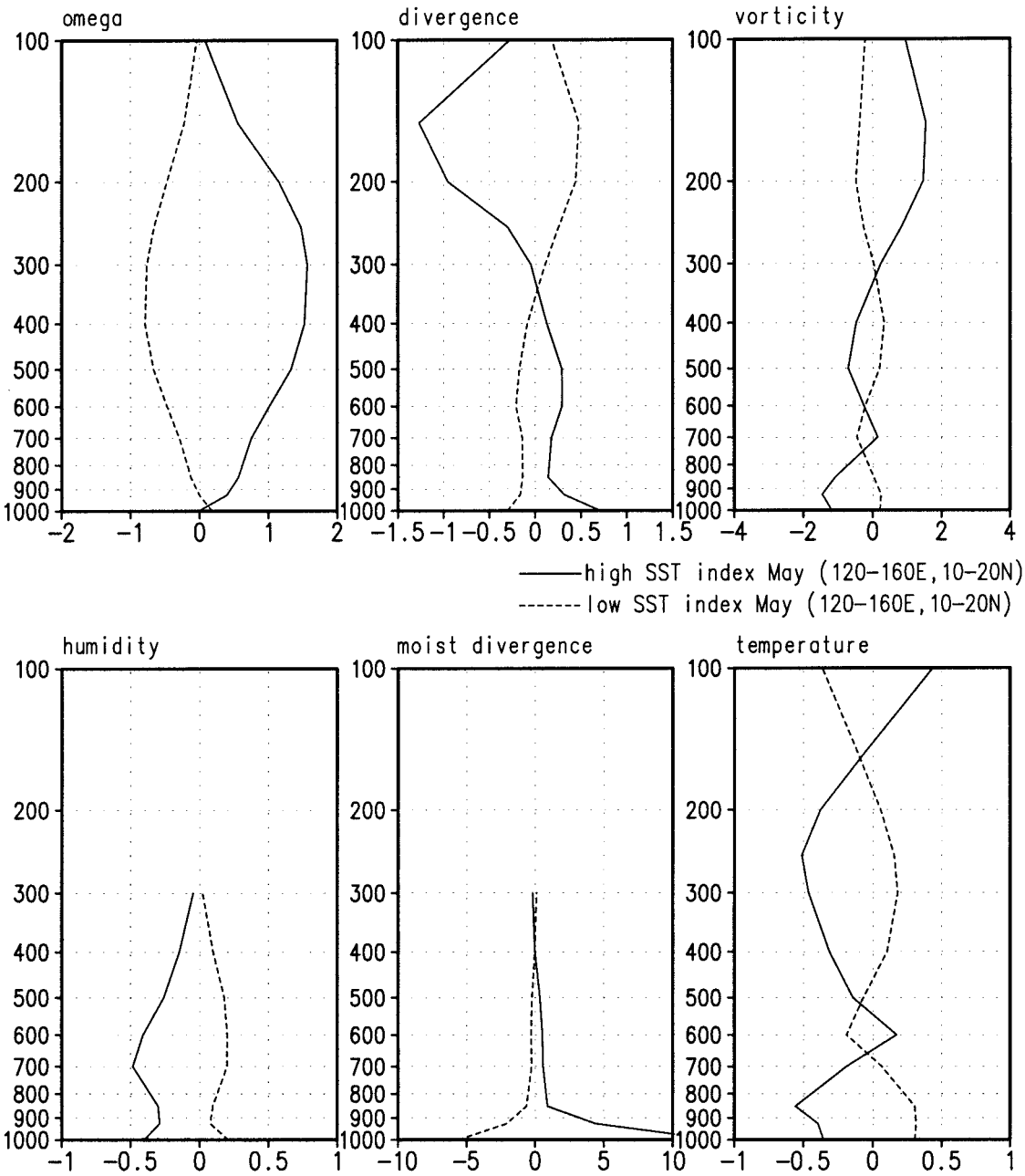

FIG. 6. Area-mean anomalies of vertical p velocity (10^{-2} Pa s^{-1}), divergence (10^{-6}), vorticity (10^{-6} s^{-1}), specific humidity (g kg^{-1}), moisture divergence (10^{-6} g kg^{-1} s^{-1}), and temperature (K) in May over 10°–20°N, 120°–160°E for high (solid curves) and low (dashed curves) SST index years. The vertical coordinate is pressure in hPa. The data used are derived from NCEP–NCAR reanalysis.

migration of the convection zone is delayed (advanced) in late spring to summer in the high (low) SST index years.

7. Results of numerical experiments

a. The atmospheric general circulation model and the experimental design

In order to understand how the SST anomalies affect the monsoon onset in the WNP, numerical experiments were performed with the atmospheric general circulation model (AGCM) developed jointly by the Center for Climate System Research (CCSR) of the University of Tokyo and the National Institute for Environmental Studies (NIES). A detailed description of the model dynamics and physics can be found in Numaguti et al. (1997). Shen et al. (1998) gave a brief discussion of the model physical schemes.

In this study, the T21 version of the model with 20 vertical levels is used. The model is integrated from an

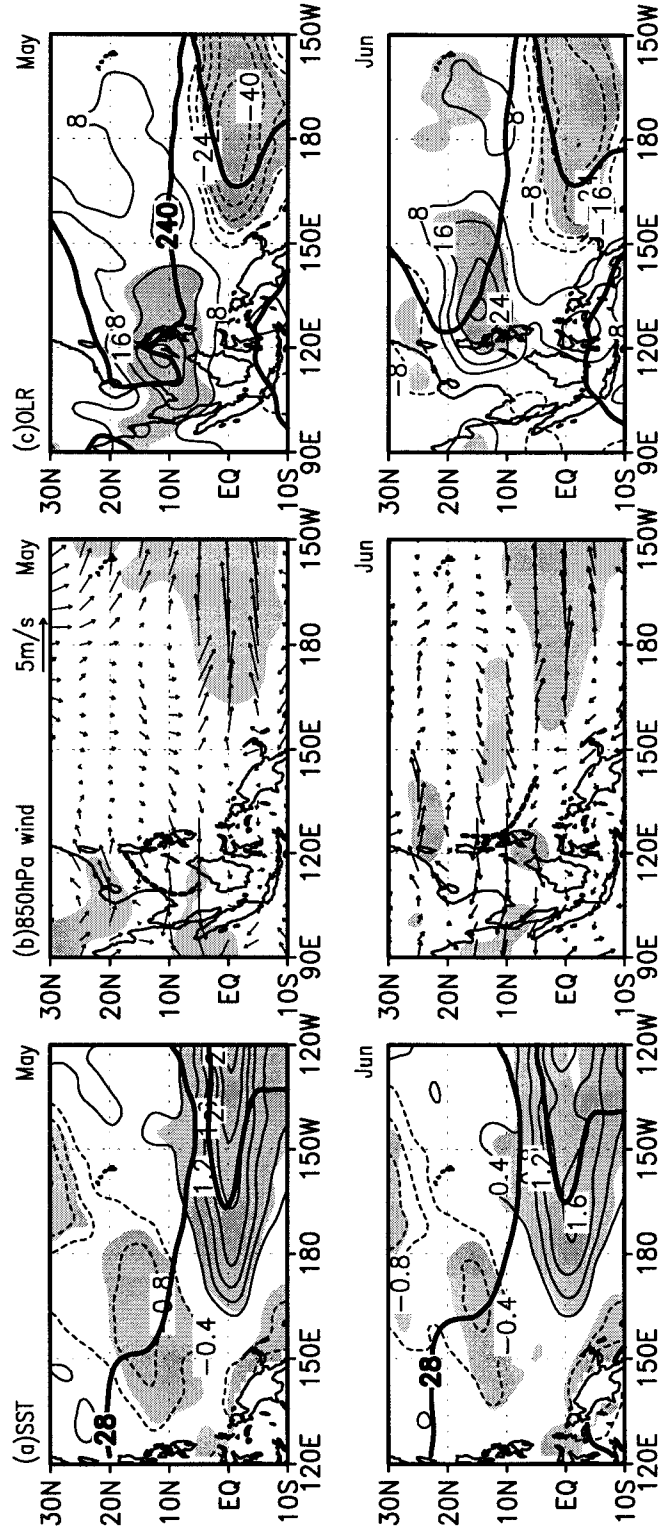

FIG. 7. Differences of (a) SST, (b) 850-hPa winds, and (c) OLR between high and low SST index years. Shading indicates regions of difference over 95% confidence level according to the Student's t-test. Thick contours in (a) are for SST of 28°C in climatology. Thick dashed lines in (b) represent the location of the monsoon trough in climatology. Thick contours in (c) are for OLR of 240 W m^{-2} in climatology.

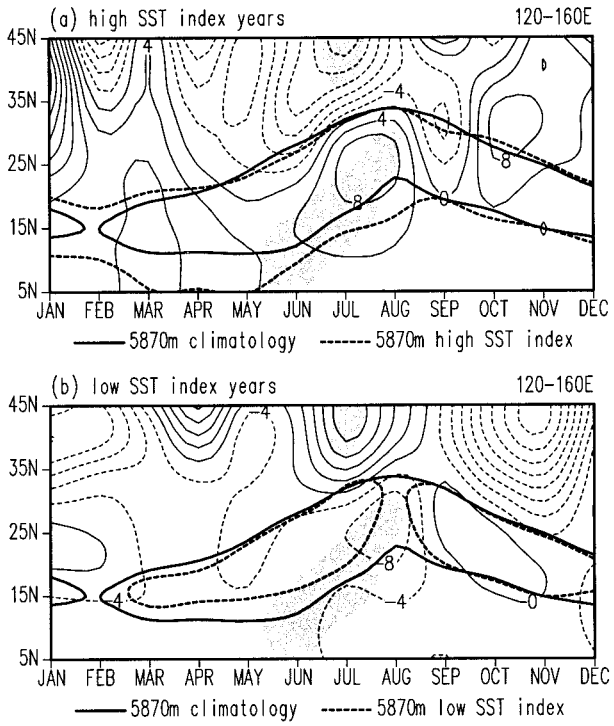

FIG. 8. Geopotential height anomalies (m) at 500 hPa along 120°–160°E for (a) high and (b) low SST index years. The thick contours are for 5870 m of monthly means. Shading indicates that the difference between high and low SST index years is significant over 95% confidence level.

isothermal atmosphere for 3 yr with Atmospheric Model Intercomparison Project (AMIP) climatological monthly mean SST. All experiments start from 1 January of the fourth year and the model is integrated for 12 months with a time step of 40 min under specified SST forcing. The instantaneous SST at each time step is interpolated from the adjacent two monthly mean SSTs.

The model reproduces reasonably well the large-scale features of precipitation and circulation in summer, captures the seasonal march of the monsoon in South Asia, and simulates the interannual variability of the broad-scale monsoon circulation comparable to the observation (Shen et al. 1998). The major deficiencies of the model include excessive summer rainfall (Shen et al. 1998), excessively high cloud and low OLR in the subtropical WNP (Numaguti et al. 1997), an eastward intrusion of lower-level westerlies in the WNP, and excessively strong lower-level westerlies and upper-level easterlies in the tropical South Asia (Shen et al. 1998). Regardless of these caveats, the model is able to capture the stepwise advance of the monsoon onset and simulate the interannual variation of transition of the convection zone in the WNP (Wu 1999). Therefore, the model is suitable for testing the sensitivity of the WNPSM onset to SST anomalies with some cautions applied.

A number of numerical experiments were designed to identify the processes by which SST anomalies affect the WNPSM onset. In the control experiment, climatological AMIP monthly mean SST is specified over the global ocean. In the warm (cold) case, monthly mean SST anomalies during the El Niño (La Niña) decay years are added to the climatological monthly mean SST over the tropical Pacific Ocean (30°S–30°N). The SST anomaly patterns associated with El Niño and La Niña decay phases from January to December were constructed from Reynolds monthly mean SST during 1950–92. Six warm events (1958, 1966, 1973, 1983, 1987, and 1992) and four cold events (1971, 1974, 1985, and 1989) were chosen, respectively, for the SST anomaly composite in the warm and cold cases. The anomalies outside the tropical Pacific were removed artificially to isolate the effects of tropical Pacific SST anomalies. To reduce the spurious SST gradients at the north and south sides of the tropical Pacific, the SST anomalies at the two grids near 30°N and 30°S were modified to one-third or two-thirds of the original values. Figure 9 shows the SST anomaly pattern for March–May mean.

b. Model onsets over the WNP in the warm and cold cases

In the control experiment, the appearance of low OLR and lower-level westerlies in the WNP is observed around mid-May (Fig. 10a). In the warm case, the corresponding occurrence of low OLR and 850-hPa westerly winds is delayed to early to mid-June (Fig. 10b). In the cold case, the low OLR and 850-hPa westerly winds in the WNP appear earlier in late April to early May (Fig. 10c). The simulated anomalous onset is consistent with observation. Note, however, in all three cases the onset is earlier than the corresponding observation by about half to one month.

To demonstrate the atmospheric response to the anomalous SST forcing, we show in Fig. 11 the area-mean anomalies of dynamic and thermal variables in the WNP in May. In the warm case, there are deep downward motion anomalies over the WNP. Convergence and cyclonic vorticity anomalies are found at upper levels and divergence and anticyclonic vorticity anomalies at lower levels. Large moisture divergence anomalies are present in the boundary layer. The humidity is lower than normal, especially between 850 and 500 hPa, mainly due to anomalous lower-level moisture divergence based on the moisture budget. The temperature anomalies increase with height below 700 hPa. The vertical profiles of moisture and temperature indicate a reduction of convective instability. Comparison of 500-hPa geopotential height anomalies indicates the WNP subtropical high is stronger and located at a lower latitude compared to the climatology case (figures not shown). In the cold case, the anomalies are basically of opposite features. The simulated large-scale circulation and thermodynamic changes in the WNP agree quite well with observations. The consistencies suggest the

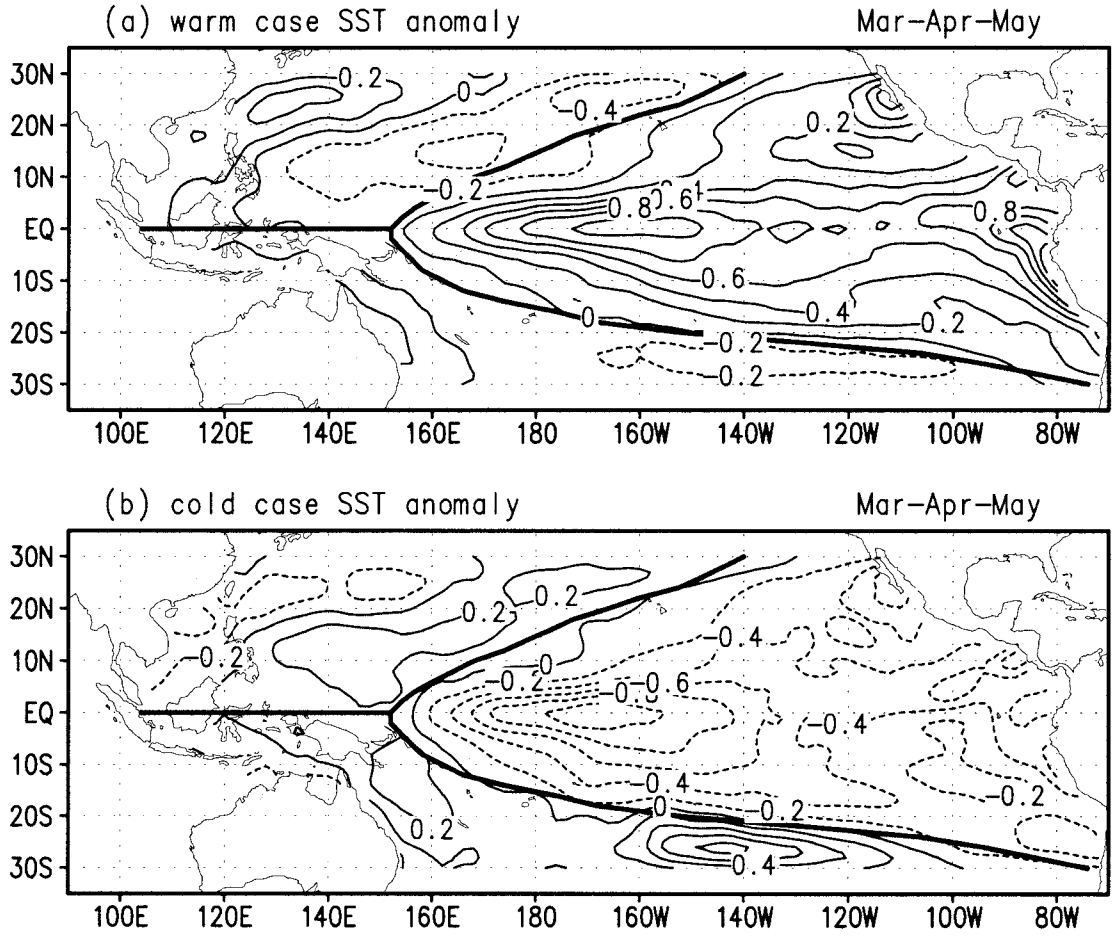

FIG. 9. Mean SST anomaly pattern in Mar–Apr–May used for the model (a) warm and (b) cold cases.

essential role of the tropical Pacific SST anomaly pattern in the interannual variation of the WNPSM onset.

c. Roles of SST anomalies in various regions of the tropical Pacific

The processes through which the tropical Pacific SST anomalies affect the large-scale circulation in the WNP were discussed by Wang et al. (2000). In response to the basinwide SST anomalies in the mature phase of El Niño, a massive anomalous surface anticyclone forms in the Philippine Sea as a Rossby wave response to the in situ suppressed heating due to negative SST anomalies in the WNP. The WNP wind anomalies are intensified by the enhanced heating due to the major warming in the equatorial eastern-central Pacific. In the WNP, the negative SST and anticyclonic anomalies can be maintained by local air–sea interaction and persist from boreal winter through the following spring. In this section, we assess the relative roles of the remote SST forcing in the equatorial eastern-central Pacific and the local SST forcing in the WNP in generation of the WNP anomalies in boreal spring and summer.

In the El Niño decay phase, when only the positive SST anomalies in the eastern-central Pacific are imposed in the SST forcing, the occurrence of low OLR in the WNP is around early June (figure not shown). When only the SST anomalies in the WNP are added, the low OLR sets in quite late around 5°–15°N, delayed to late June. Late appearance of persistent lower-level westerlies can be seen for both cases. Thus, both positive SST anomalies in the eastern-central Pacific and weaker negative SST anomalies in the WNP can effectively cause a delayed onset of the WNPSM.

When only the warm SST anomalies in the eastern-central Pacific are retained, the vertical profiles of vertical motion, divergence, and vorticity anomalies resemble those in the warm case (Fig. 12 vs Fig. 11). The magnitude of vertical motion and divergence anomalies are somewhat weaker. The stratification change below 700 hPa is less clear compared to the warm case. On the other hand, when only the SST anomalies in the WNP are retained, there are noticeable anomalies of vorticity, vertical motion, and divergence at lower levels. The humidity and temperature anomalies at lower levels are closer to the warm case. The results suggest

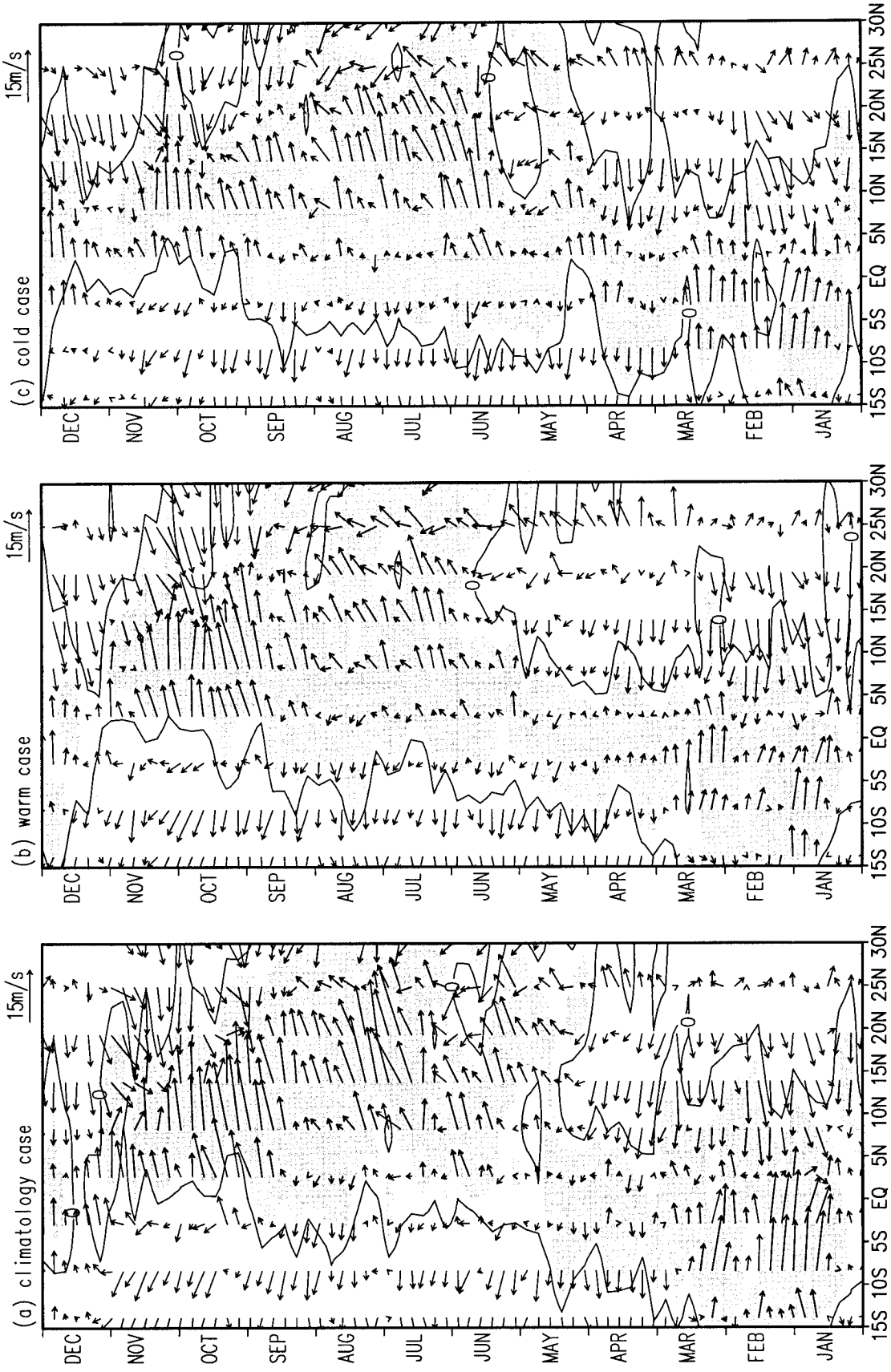

FIG. 10. OLR along 120°–160°E and 850-hPa wind along 110°–150°E for (a) model climatology, (b) warm, and (c) cold cases. The contours are for OLR of 220 W m^{-2}. Shading denotes OLR less than 200 W m^{-2}.

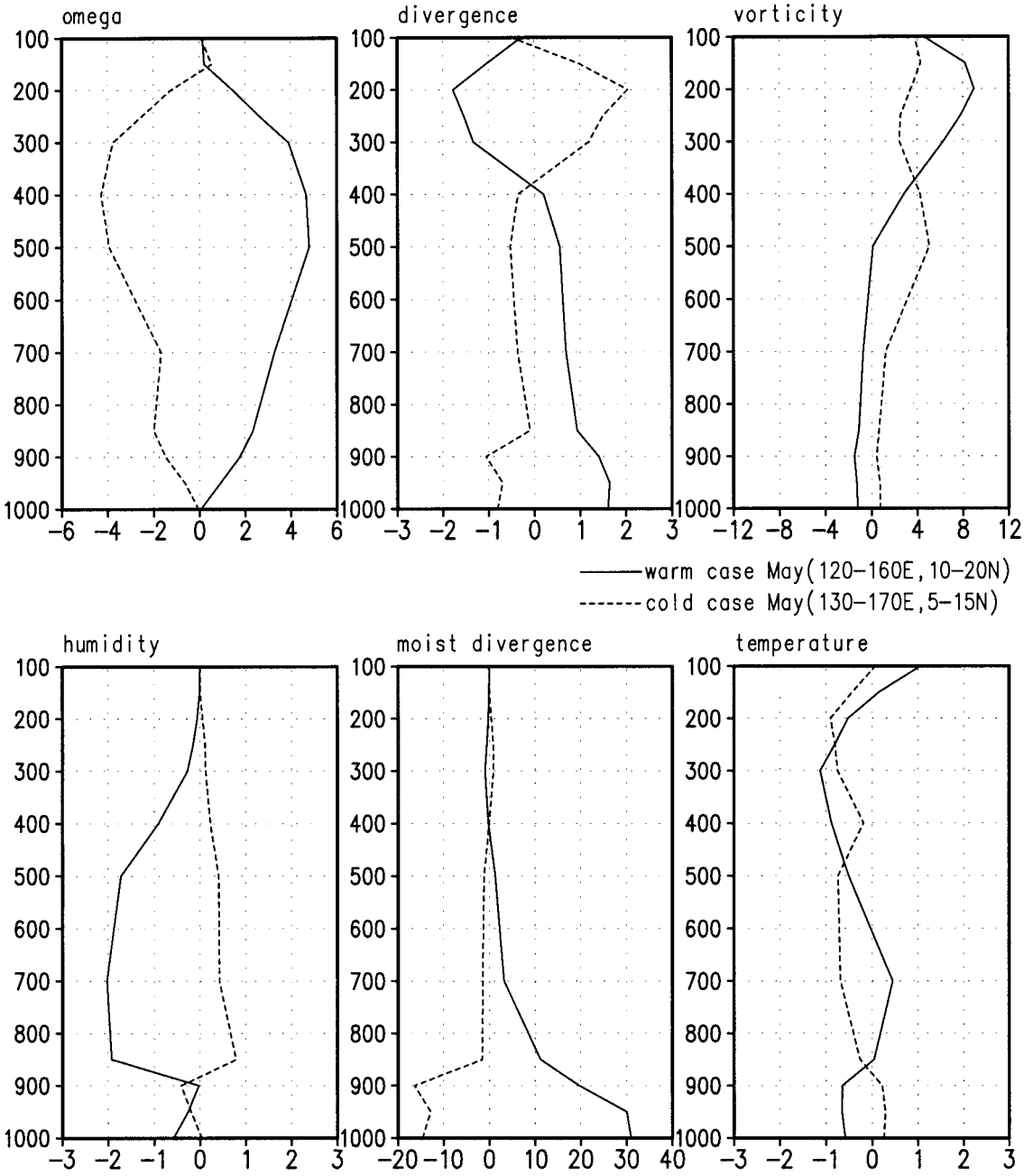

FIG. 11. The same as Fig. 6 except that the results are derived from numerical experiments for the model warm case over 10°–20°N, 120°–160°E (solid curves) and cold case over 5°–15°N, 130°–170°E (dashed curves). A slight different area was chosen for the cold case considering the southeastward shift of the upper-level divergent wind anomalies and the lower-level anomalous cyclone over the WNP.

that the remote SST forcing play a dominant role in generating the upper-level convergence and deep downward motion anomalies in the WNP. The local SST forcing is more effective than the remote SST forcing in reducing the convective instability. Both remote and local forcing contribute to the development of the lower-level divergence and downward motion.

In the La Niña decay phase (figures not shown), the SST anomalies in the WNP or eastern-central Pacific alone do not produce an earlier onset. This suggests that the SST anomaly contrast between the WNP and the equatorial central Pacific, rather than the local SST or remote SST anomalies alone, is responsible for the anomalous onset. The cold SST anomalies in the eastern-central Pacific are also not as effective as the warm SST anomalies in producing large-scale circulation and

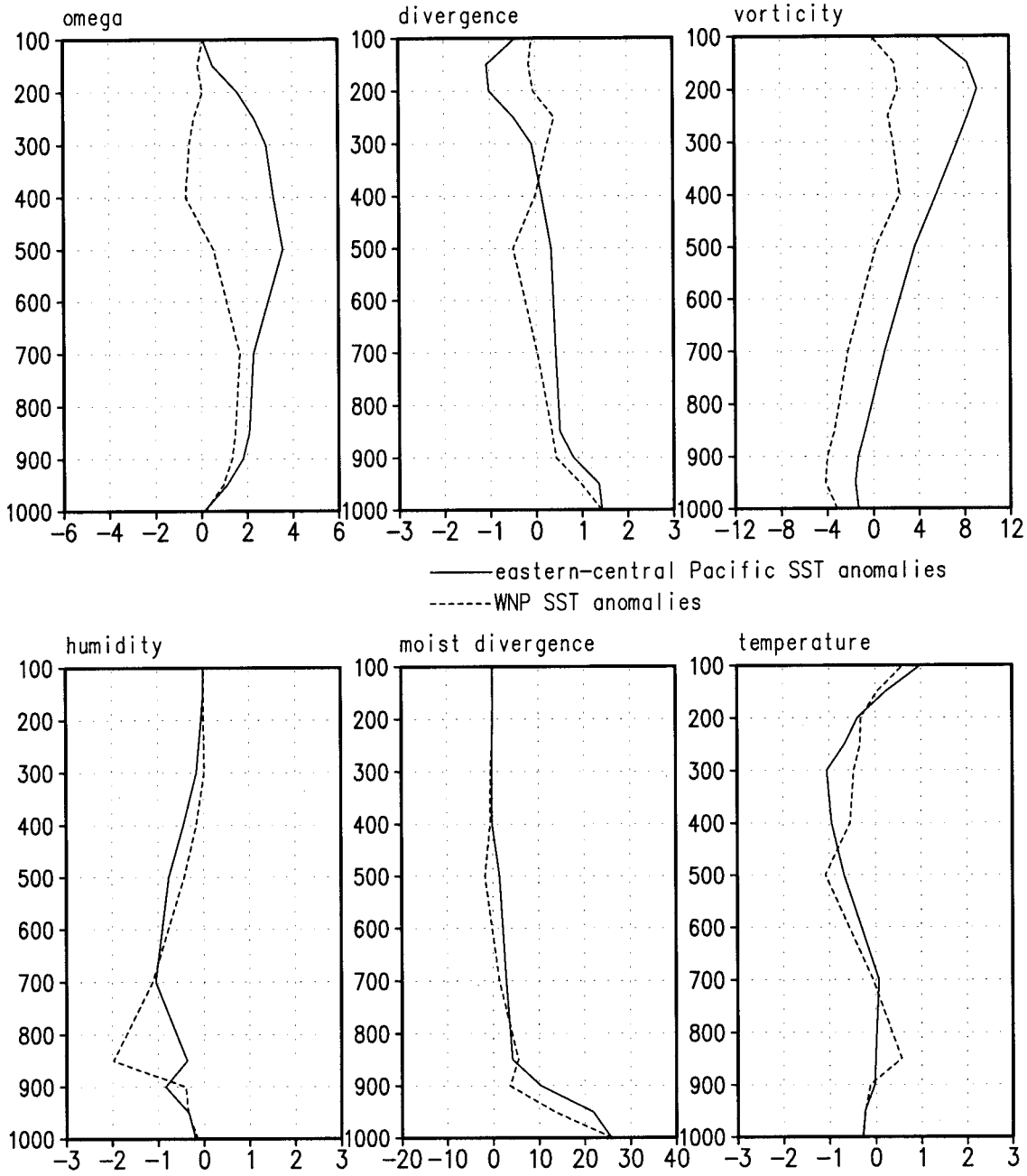

FIG. 12. Similar to the model warm case in Fig. 11 but the anomalous SST forcing differs. The solid (dashed) curves represent the results derived from the experiment in which only the eastern-central Pacific (WNP) SST anomalies are retained. The eastern-central Pacific (WNP) refers to the region to the east (west and north) of the thick lines in Fig. 9.

thermodynamic anomalies in the WNP. In particular, the vertical motion and upper-level vorticity anomalies and the humidity and moisture convergence anomalies near the surface are much weaker compared to the El Niño counterpart. When only the SST anomalies in the WNP are retained, the induced circulation and thermodynamic anomalies have magnitudes comparable to the El Niño counterpart. Thus, the in situ warm SST anomalies in the WNP during La Niña decay phase can effectively change the lower-level circulation and convective instability.

8. Summary and discussion

The climatological monsoon rain in the SCS and WNP exhibits multiple onsets. The onset consists of three distinct stages. The SCS summer monsoon onset in mid-May is the earliest in the SCS and WNP. Sub-

sequent onset over the southwestern Philippine Sea in mid-June is nearly concurrent with the onset of Mei-yu (Baiu) in east Asia. The last onset stage in mid–late July in the northeastern part of the WNP concurs with the end of Mei-yu (Baiu) and the second northward jump of the subtropical rainband in East Asia. These linkages have been shown to a part of the climatological ISO in the Northern Hemisphere summer monsoon domain (Wang and Xu 1997).

The interannual variability of the onset in the WNP is about 2–3 times of that in the Indian monsoon region. The standard deviation of the onset increases eastward from 3 pentads in the SCS to more than 5 pentads east of 150°E. The onset is determined by both the seasonal cycle and the ISO. In the Indian monsoon region, the onset variability is largely attributed to the ISO. In the central SCS, the seasonal cycle and the ISO have comparable contributions to the onset variability. In the WNP, the seasonal cycle transition has large year-to-year variation and is a dominant source for the onset variability.

The most significant result from the data analysis is that the interannual variation of the onset in the WNP displays a nearly in-phase variation pattern and it is highly correlated with the SST difference between the equatorial central Pacific and the WNP in the previous winter and spring. This implies that in majority of the cases, the delayed (advanced) monsoon onset in the WNP follows the mature phases of El Niño (La Niña).

The large-scale SST anomaly pattern in the tropical Pacific affects the WNPSM onset through modifying the large-scale circulation and thermodynamics in the WNP. During the El Niño decay phase, the anomalous heating due to warm SST anomalies in the equatorial central Pacific induces anomalous upper-level convergence, descent, and lower-level divergence over the WNP. The cold SST anomalies in the WNP reduce the lower-level moisture and convective instability through reduction of surface heat fluxes and lower-level moisture divergence. As a result, lower-level anomalous anticyclone forms through a Rossby wave response to suppressed heating. Through induced atmospheric circulation anomalies and thermodynamic changes, the seasonal migrations of the monsoon trough, the western Pacific subtropical high, and the convection zone are delayed in spring and early summer. This leads to a late seasonal transition from the dry to wet phase in the WNP, which reflects a late setup of large-scale circulation and thermodynamics for the development of convection. The latter, in turn, causes a late onset of the WNPSM. Similar processes work in La Niña decay phase except with opposite anomalies.

Following the mature phase of El Niño or La Niña, the large-scale SST anomaly pattern in the tropical Pacific usually persists from winter to spring. In this sense, the winter SST anomaly pattern has prediction value. The SST anomaly in the WNP is normally highly related to ENSO. There are exceptions. For example, in spring of 1994 during the development of 1994 warm event, the SST anomalies in the WNP were positive, different from the typical El Niño SST anomaly pattern after the mature phase. This leads to a slightly negative SST index and an early onset in the WNP.

According to the sensitivity experiments, warm SST anomalies in the equatorial eastern-central Pacific are dominant in inducing upper-level divergence and vertical motion anomalies in the WNP. Local negative SST anomalies have a larger contribution to the formation of lower-level anticyclonic wind anomalies and the reduction of convective instability. On the other hand, the cold SST anomalies in the equatorial eastern-central Pacific are less effective than the warm SST anomalies in inducing large-scale circulation changes related to the WNPSM onset. In contrast, the warm SST anomalies in the WNP are more effective in causing lower-level circulation anomalies and changes of convective instability.

Because of the low horizontal resolution (T21) used in the model experiments, the numerical results may only be suggestive. Previous studies (e.g., Sperber et al. 1994; Stephenson et al. 1998; Martin 1999) discussed the dependence of the monsoon simulation on the model horizontal resolution. Some simulated features become more realistic with increasing resolution. However, not all features improve with increased resolution. The large-scale distribution of precipitation in the monsoon region does not necessarily become better at the higher resolution.

Although the numerical results may depend on the model used and have limitations due to the low horizontal resolution, we believe that the results obtained in this study are meaningful in a qualitative sense. The robustness of the numerical results is supported by sensitivity tests in which the initial conditions are changed. Two extra experiments were done with January SST anomalies suppressed. The results show that after the suppression of SST anomalies in January, the appearance of low OLR and westerly winds in the WNP remains delayed (advanced) in the warm (cold) case. This indicates that qualitatively, the WNPSM onset is not sensitive to the changes of the initial conditions. Soman and Slingo (1997) did similar experiments of sensitivity to initial conditions. Their results indicate that the initial conditions have little effect on the onset of the South Asian monsoon and suggest that the SST anomalies are the controlling factor for the interannual variation of the onset. Shukla (1998) showed that the wind patterns and rainfall in certain regions of the Tropics are strongly determined by the temperature of the underlying sea surface so that they do not show sensitive dependence on the initial conditions of the atmosphere. According to Ferranti et al. (1997), when the SST forcing in the preceding spring is large (e.g., 1983, 1987, and 1988), the large-scale circulation anomalies in summer are less spread in the ensemble experiments.

The experiments with regional SST anomalies give

some idea on the magnitudes of the atmospheric anomalies caused by regional SST anomalies. The atmospheric anomalies due to the full SST forcing, however, are not a linear superposition of those anomalies caused by the remote-only and local-only SST forcing, indicating that the remotely forced and locally forced anomalies can interact with each other.

This study focuses on the role of tropical Pacific SST anomalies in the interannual variation of the WNPSM onset. Other possible factors are not addressed. These factors include the land–sea thermal contrast between the Asian continent and the western Pacific, the land surface hydrological processes in the Asian continent, the SST anomalies in the Indian Ocean and extratropical North Pacific, and the thermal anomalies over Australia. Although we believe that these factors are less important than the tropical Pacific SST anomalies, further studies are needed to assess their roles on the seasonal evolution of convection and large-scale circulation and their influence on the interannual variation of the WNPSM onset.

Acknowledgments. The authors acknowledge the use of the CCSR/NIES AGCM in the numerical experiments. This study is supported by NSF Climate Dynamic Program, NOAA/OGP under GOALS and PACS Program, and ONR Marine Meteorology Program. The authors appreciate the comments from Drs. R. Lukas and N. Nicholls and two anonymous reviewers. This is the School of Ocean and Earth Science and Technology Publication No. 5208 and International Pacific Research Center Publication No. 46. International Pacific Research Center is sponsored in part by the Frontier Research System for Global Change.

REFERENCES

Chelliah, M., and P. Arkin, 1992: Large-scale interannual variability of monthly outgoing longwave radiation anomalies over the global tropics. *J. Climate,* **5,** 371–389.

Das, P. K., 1987: Short- and long-range monsoon prediction in India. *Monsoons,* J. S. Fein and P. L. Stephens, Eds., John Wiley and Sons, 549–578.

Drosdowsky, W., 1996: Variability of the Australia summer monsoon at Darwin: 1957–1992. *J. Climate,* **9,** 85–96.

Ferranti, L., J. M. Slingo, T. N. Palmer, and B. Hoskins, 1997: Relations between interannual and intraseasonal monsoon variability as diagnosed from AMIP integrations. *Quart. J. Roy. Meteor. Soc.,* **123,** 1323–1357.

Gadgil, S., P. V. Joseph, and N. V. Joshi, 1984: Ocean–atmosphere coupling over monsoon regions. *Nature,* **312,** 141–143.

——, A. Guruprasad, and J. Srinivasan, 1992: Systematic bias in the NOAA outgoing longwave radiation dataset? *J. Climate,* **5,** 867–875.

Graham, N. E., and T. P. Barnett, 1987: Sea surface temperature, surface wind divergence, and convection over tropical oceans. *Science,* **238,** 657–659.

Gruber, A., and A. F. Krueger, 1984: The status of the NOAA outgoing longwave radiation date set. *Bull. Amer. Meteor. Soc.,* **65,** 958–962.

Hendon, H. H., N. E. Davidson, and B. Gunn, 1989: Australian summer monsoon onset during AMEX 1987. *Mon. Wea. Rev.,* **117,** 370–390.

Huang, R.-H., and Y.-F. Wu, 1989: The influence of ENSO on the summer climate change in China and its mechanism. *Adv. Atmos. Sci.,* **6,** 21–32.

Indian Meteorological Department, 1943: *Climatological Atlas for Airmen.* Indian Meteorological Department, 100 pp.

Ji, M., A. Leetmaa, and J. Derber, 1995: An ocean analysis system for seasonal to interannual climate studies. *Mon. Wea. Rev.,* **123,** 460–481.

Joseph, P. V., B. Liebmann, and H. H. Hendon, 1991: Interannual variability of the Australian summer monsoon onset: Possible influence of Indian summer monsoon and El Niño. *J. Climate,* **4,** 529–538.

——, J. K. Eischeid, and R. J. Pyle, 1994: Interannual variability of the onset of the Indian summer monsoon and its association with atmospheric features, El Niño, and sea surface temperature anomalies. *J. Climate,* **7,** 81–105.

Ju, J., and J. M. Slingo, 1995: The Asian summer monsoon and ENSO. *Quart. J. Roy. Meteor. Soc.,* **121,** 1133–1168.

Kalnay, E., and Coauthors, 1996: The NCEP/NCAR 40-year reanalysis project. *Bull. Amer. Meteor. Soc.,* **77,** 437–471.

Lau, K.-M., and S. Yang, 1997: Climatology and interannual variability of the southeast Asian summer monsoon. *Adv. Atmos. Sci.,* **14,** 141–162.

Livezey, R. E., and W. Y. Chen, 1983: Statistical field significance and its determination by Monte Carlo techniques. *Mon. Wea. Rev.,* **111,** 46–59.

Martin, G. M., 1999: The simulation of the Asian summer monsoon, and its sensitivity to horizontal resolution, in the U. K. Meteorological Office Unified model. *Quart. J. Roy. Meteor. Soc.,* **125,** 1499–1525.

Matsumoto, J., 1997: Seasonal transition of summer rainy season over Indochina and adjacent monsoon region. *Adv. Atmos. Sci.,* **14,** 231–245.

Murakami, T., and J. Matsumoto, 1994: Summer monsoon over the Asian continent and western North Pacific. *J. Meteor. Soc. Japan,* **72,** 719–745.

——, L.-X. Chen, and A. Xie, 1986: Relationship among seasonal cycles, low-frequency oscillations, and transient disturbances as revealed from outgoing longwave radiation data. *Mon. Wea. Rev.,* **114,** 1456–1465.

Nitta, T., 1987: Convective activities in the tropical western Pacific and their impacts on the Northern Hemisphere summer circulation. *J. Meteor. Soc. Japan,* **65,** 165–171.

Numaguti, A., M. Takahashi, T. Nakajima, and A. Sumi, 1997: Description of CCSR/NIES atmospheric general circulation model. *Study on the Climate System and Mass Transport by a Climate Model. CGER's Supercomputer Monogr. Report,* Vol. 3, National Institute for Environmental Studies, Environment Agency of Japan, 1–48.

Reynolds, R. W., and T. Smith, 1994: Improved global sea surface temperature analysis using optimum interpolation. *J. Climate,* **7,** 929–948.

Shen, S., and K.-M. Lau, 1995: Biennial oscillation associated with the East Asian summer monsoon and tropical sea surface temperatures. *J. Meteor. Soc. Japan,* **73,** 105–124.

Shen, X.-S., M. Kimoto, and A. Sumi, 1998: Role of land surface processes associated with interannual variability of broad-scale Asian summer monsoon as simulated by the CCSR/NIES AGCM. *J. Meteor. Soc. Japan,* **76,** 217–236.

Shukla, J., 1988: Predictability in the midst of chaos: A scientific basis for climate forecasting. *Science,* **282,** 728–731.

Smith, T. M., R. W. Reynolds, R. E. Livezey, and D. C. Stokes, 1996: Reconstruction of historical sea surface temperatures using empirical orthogonal functions. *J. Climate,* **9,** 1403–1402.

Soman, M. K., and J. M. Slingo, 1997: Sensitivity of Asian summer monsoon to aspects of sea surface temperature anomalies in the tropical Pacific Ocean. *Quart. J. Roy. Meteor. Soc.,* **123,** 309–336.

Sperber, K. R., S. Hameed, G. L. Potter, and J. S. Boyle, 1994: Simulation of the northern summer monsoon in the ECMWF model: Sensitivity to horizontal resolution. *Mon. Wea. Rev.,* **122,** 2461–2481.

Stephenson, D.-B., F. Chauvin, and J. F. Royer, 1998: Simulation of the Asian summer monsoon and its dependence on model horizontal resolution. *J. Meteor. Soc. Japan,* **76,** 237–265.

Tanaka, M., 1992: Intraseasonal oscillation and the onset and retreat dates of the summer monsoon over East, Southeast Asia and the western Pacific region using GMS high cloud amount data. *J. Meteor. Soc. Japan,* **70,** 613–629.

——, 1997: Interannual and interdecadal variations of the western North Pacific monsoon and the East Asian Baiu rainfall and their relationship to ENSO cycles. *J. Meteor. Soc. Japan,* **75,** 1109–1123.

Waliser, D. E., and W. Zhou, 1997: Removing satellite equatorial crossing time biases from the OLR and HRC datasets. *J. Climate,* **10,** 2125–2146.

Wang, B., 1994: Climatic regimes of tropical convection and rainfall. *J. Climate,* **7,** 1109–1118.

——, and R. Wu, 1997: Peculiar temporal structure of the South China Sea summer monsoon. *Adv. Atmos. Sci.,* **14,** 177–194.

——, and X. Xu, 1997: Climatological intraseasonal oscillation in the western North Pacific. *J. Climate,* **10,** 1071–1085.

——, R. Wu, and X. Fu, 2000: Pacific–East Asian teleconnection: How does ENSO affect East Asian climate? *J. Climate,* **13,** 1517–1536.

Wu, R., 1999: Interannual variability of summer monsoon onset over the western North Pacific. Ph.D. dissertation, Department of Meteorology, University of Hawaii at Manoa, 251 pp. [Available from Department of Meteorology, University of Hawaii at Manoa, 2525 Correa Road, HIG, Honolulu, HI 96822.]

Xie, P., and P. A. Arkin, 1997: Global precipitation: A 17-year monthly analysis based on gauge observations, satellite estimates, and numerical outputs. *Bull. Amer. Meteor. Soc.,* **78,** 2539–2558.

——, and ——, 1998: Global monthly precipitation estimates from satellite-observed outgoing longwave radiation. *J. Climate,* **11,** 137–164.

Yan, J.-Y., 1997: Observational study on the onset of the South China Sea southwest monsoon. *Adv. Atmos. Sci.,* **14,** 277–287.